# Photorefractive Properties of Undoped and Doped Single Crystal SBN:60

George A. Rakuljic, Amnon Yariv, Ratnakar Neurgaonkar

George A. Rakuljic, Amnon Yariv, Ratnakar Neurgaonkar, "Photorefractive Properties of Undoped and Doped Single Crystal SBN:60," Proc. SPIE 0567, Advances in Materials for Active Optics, (4 March 1986); doi: 10.1117/12.949825

SPIE.

Event: 29th Annual Technical Symposium, 1985, San Diego, United States

# Photorefractive Properties of Undoped and Doped Single Crystal SBN:60

George A. Rakuljic and Amnon Yariv

Department of Applied Physics, California Institute of Technology
Pasadena, California 91125

Ratnakar Neurgaonkar
Science Center, Rockwell International Corporation
Thousand Oaks, California 91360

## Abstract

We present the results of our theoretical and experimental studies of the photorefractive effect in single crystal SBN:60, SBN:Ce, and SBN:Fe. Specifically, the two-beam coupling coefficients, response times and absorption coefficients of these materials are given.

## Introduction

A given photorefractive material is considered useful for optical processing applications such as phase conjugate optics if it possesses three important features: low response time, large coupling coefficient and high optical quality. Speed is necessary if the crystal is to be used in real-time applications, while large photorefractive coupling is required for the construction of efficient devices. However, a crystal with poor optical quality is of little practical importance, regardless of its speed and gain. Although a material is yet to be found which completely satisfies all three requirements, here we show how well SBN:60 approximates these properties.

## Material Properties

Strontium barium niobate (SBN) belongs to a class of tungsten bronze ferroelectrics which is pulled from a solid solution of alkaline earth niobates. The crystal is transparent and can be grown with a variety of ferroelectric and electrooptic properties depending on the specific cation ratios introduced into the structure. In SBN the unit cell contains ten $NbO_6$ octahedra with only five alkaline earth cations to fill ten interstitial sites.[1,2,3] The structure is thus incompletely filled which permits the addition of a wide range of dopants into the host crystal. The general formula for SBN is $Sr_xBa_{1-x}Nb_2O_6$ so that SBN:60 represents $Sr_{.6}Ba_{.4}Nb_2O_6$.

The point group symmetry of SBN is 4mm which implies that its electrooptic tensor is non-zero. The dominant electrooptic coefficient is $r_{33}$ which ranges from 100 pm/V in SBN:25 to 1400 pm/V in SBN:75. SBN:75 would, therefore, appear to be the best photorefractive SBN crystal were it not for the fact that optical quality diminishes with increasing Sr concentration. Hence, SBN:60 was selected as the candidate SBN photorefractive material on the basis of its high optical quality and moderately large electrooptic coefficient.

## Photorefractive Properties

Single crystals of SBN:60, SBN:Ce ($Sr_{.6}Ba_{.4}Nb_2O_6$:Ce) and SBN:Fe ($Sr_{.6}Ba_{.4}Nb_2O_6$:Fe) grown at Rockwell International Corporation were studied using the two-wave mixing experiment shown in Fig. 1 to determine their effectiveness as photorefractive media. In Fig. 1 beams 1 and 2 are plane waves which intersect in the crystal and thus form an intensity interference pattern. Charge is excited by this periodic intensity distribution into the conduction band, where it migrates under the influence of diffusion and drift in the internal electric field, and then preferentially recombines with traps in regions of low irradiance. A periodic space charge is thus created which modulates the refractive index via the electrooptic effect. This index grating, being out of phase with the intensity distribution, introduces an asymmetry that allows one beam to be amplified by constructive interference with light scattered by the grating, while the other beam is attenuated by destructive interference with diffracted light. This process is shown graphically in Fig. 2.

Mathematically, this two-beam coupling may be described in the steady-state as follows:

$$\frac{dI_1}{d\xi} = -\Gamma \frac{I_1 I_2}{I_1 + I_2} - \alpha I_1$$

$$\frac{dI_2}{d\xi} = \Gamma \frac{I_1 I_2}{I_1 + I_2} - \alpha I_2$$

where $I_1$, $I_2$ are the intensities of beams 1 and 2 inside the crystal respectively, $\Gamma$ is the two-beam coupling coefficient, $\alpha$ is the absorption coefficient and $\xi \equiv z/\cos\theta_i$ where $0 \leq \xi \leq \equiv d/\cos\theta_i$. The transient behavior is modeled by the following:

$$I_i(\xi;t) = (1 - e^{-t/\tau}) I_i(\xi;t \to \infty) + e^{-t/\tau} I_i(\xi;t = 0), \quad i = 1, 2$$

where $\tau$ is a characteristic time constant and

$$I_i(\xi;t \to \infty) \equiv I_i(\xi).$$

The solutions of the above coupled wave equations are

$$I_1(\ell) = \frac{[I_1(0) + I_2(0)]e^{-\alpha\ell}}{1 + \frac{I_2(0)}{I_1(0)} e^{\Gamma\ell}}$$

$$I_2(\ell) = \frac{[I_1(0) + I_2(0)]e^{-\alpha\ell}}{1 + \frac{I_1(0)}{I_2(0)} e^{-\Gamma\ell}}$$

By measuring the four intensities $I_1(0)$, $I_2(0)$, $I_1(\ell)$, and $I_2(\ell)$, both in the steady-state and as a function of time, the two-beam coupling coefficient $\Gamma$ and the response time $\tau$ can, therefore, be obtained from the above equations.

Maximum coupling will result in crystals with large $\Gamma$ but small $\alpha$. However, $\alpha$ and $\Gamma$ are not independent. In fact, since charge must first be excited into a conduction band by the intensity interference pattern in order to start the photorefractive process, some absorption is necessary. This is precisely where the role of the dopant enters. By purposely introducing impurities into the crystal, donor sites are created which become the absorption centers. It must be noted, however, that any absorption which does not contribute to the photorefractive mechanism is undesirable.

Figures 4 and 5 show the effect of cerium and iron impurities on the absorption spectra of undoped SBN, whose spectra is given in Fig. 3. Several interesting observations can be made. For one, the band edge shifts from 400 nm in SBN to 430 nm in SBN:Ce and 500 nm in SBN:Fe. Secondly, although the SBN was not intentionally doped, there are signs of deep level impurities evidenced by perturbations in the spectra near 550 nm. Finally, the effects of Ce and Fe in SBN are seen to be significantly different. While the spectra of SBN:Ce is rather featureless with a broad deep level centered at 480 nm, the spectra of SBN:Fe displays a structured but broad absorption extending from 500 nm to 700 nm with characteristic peaks at 550 nm and 590 nm. Future investigation of these lines will indicate whether or not they contribute to the photorefractive effect.

First principle calculations using the band transport model[5] can be used to derive expressions for $\Gamma$ and $\tau$. Solutions to the photorefractive equations developed most fully by Kukhtarev[6,7,8] show that $\Gamma$ and $\tau$ can be represented functionally as follows:

$$\Gamma = \Gamma(k_g, E_o, \lambda, T; r, N_D, N_A, \varepsilon, n)$$

$$\tau = \tau(k_g, E_o, \lambda, T, I_o; s, \gamma_R, \mu, N_D, N_A, \varepsilon)$$

where the experimentally controlled variables are

$k_g$ = grating wave number

$E_o$ = applied field (normal to grating planes

$\lambda$ = wavelength of incident light

$T$ = temperature

$I_o$ = total irradiance

while the material parameters are

$r$ = effective electrooptic coefficient

$s$ = photoionization cross-section

$\gamma_R$ = two-body recombination rate

$\mu$ = mobility

$N_D$ = number of donors under dark conditions

$N_A$ = number of traps under dark conditions

$\varepsilon$ = static dielectric constant

$n$ = background refractive index

These equations were applied to cerium doped SBN. Specifically the sample contained $10^{18} cm^{-3}$ cerium atoms which resulted in an as-grown crystal with the following photorefractive parameters:

$\Gamma = 11\ cm^{-1}$

$\tau_e = 0.10$ sec

$\alpha = 1.8\ cm^{-1}$

at

$I_o = 1 W/cm^2$

$T = 298°K$

$\lambda = 0.5145\ \mu m$

$E_o = 0$ V/cm

$\lambda_g = 5\ \mu m$

Variations in $\Gamma$ and $\tau$ about this "operating point" are shown in Figs. 6-13 along with the experimentally obtained values of the two-beam coupling coefficient and response time for SBN:60 and SBN:Ce. Data for SBN:Fe is not shown since striations in the crystal so affected the optical quality of the crystal that no reliable experimental values could be measured. Although the SBN:60 and SBN:Ce samples were striation free and displayed good optical quality, to date all of the SBN:Fe crystals, regardless of their Fe concentration, were severely marked with striations. It is believed, however, that better control of the melt temperature will eliminate this problem.

With no applied field Fig. 7 indicates that $\Gamma$ should be greater than 1 $cm^{-1}$ for all practical values of $\lambda_g$, while the application of an electric field of 2 kV/cm ought to increase the coupling coefficient to 35 $cm^{-1}$ at $\lambda_g = 5\ \mu m$ as shown in Fig. 8. Such a large response would then make even very thin samples of SBN:Ce useful photorefractive media. However, in practice, these large values of $\Gamma$ are not easily obtainable. As an electric field is applied to the crystal, induced stresses deform the material and the incident beams are distorted. Therefore, we conclude that the application of an electric field to the crystal in order to control its two-beam coupling coefficient is of limited use.

Another manner in which $\Gamma$ can be modified was suggested in Ref. 9. By varying the trap density $N_A$ with reduction and oxidation treatments, one should be able to control $\Gamma$ as shown in Fig. 9. Although the exact number density of traps is difficult to measure, we have indeed been able to change the two-beam coupling coefficient from less than 0.1 $cm^{-1}$ to 15 $cm^{-1}$ by heating the crystal in atmospheres with different oxygen partial pressures.

However, the predicted variation of response time with trap density, which is shown in Fig. 10, has yet to be observed in SBN:Ce. Although $\Gamma$ decreases as expected when the crystal is heated in a reducing atmosphere, the time constant remains unchanged at a

typical value of 100 msec at 1 W/cm$^2$ irradiance. This unexpected and currently unexplained result has complicated our effort at producing a cerium doped SBN photorefractive crystal with 1 millisecond response time, since heat treatment was proposed as a method of achieving this goal.[9] Therefore, other techniques may need to be invoked in order to obtain the desired speed of response.

Figures 11, 12 and 13 show how the response time $\tau$ is affected with changes in the mobility $\mu$, the two-body recombination rate $\gamma_R$, and the photoionization cross-section s, respectively. Since $\mu$ is predominantly an intrinsic quantity of the host crystal, little can be done to increase its value. However, s and $\gamma_R$ are extrinsic parameters which can be varied by the selection of different dopants. By choosing a dopant with either a larger photoionization cross-section or a smaller two-body recombination rate coefficient than is presently obtained with cerium, the resulting doped sample of SBN should then possess a shorter response time. The selection of such a dopant, unfortunately, is a nontrivial task.

Consider Table I which shows the results of an elemental analysis by nuclear activation of undoped and cerium doped SBN. Since undoped SBN is photorefractive while containing only trace quantities of cerium, we must conclude that cerium is not the only photorefractive species for SBN. In fact, Table I indicates that there are significant amounts of Fe, Ni, Mo and Ta impurities present in the undoped SBN crystal, and Fe and Ni, for example, are known to be effective photorefractive centers in $LiNbO_3$.[10] Although iron has already been used as a dopant for SBN, the resulting crystals were optically imperfect. Therefore, we suggest that not only should the growth of iron and cerium doped SBN continue, but that crystals doped with other impurities, which may prove to have better values of $\gamma_R$ and s, should also be investigated.

## Summary of Results

A major goal of our work has been the growth of high optical quality photorefractive SBN crystals. This was accomplished in part by growing striation-free SBN:60 and SBN:Ce. In fact, optically excellent crystals of SBN:60 and SBN:Ce can now be had as cubes approaching 1 cm a side. SBN:Fe, unfortunately, has yet to be grown without striations. As was indicated earlier, even better control of the melt temperature may be necessary to eliminate this problem.

Large two-beam coupling was observed in both SBN:60 and SBN:Ce. Values of $\Gamma$ ranged from 2 cm$^{-1}$ in SBN:60 to greater than 10 cm$^{-1}$ in SBN:Ce. Such response was large enough to permit the use of these crystals in the construction of the ring[11] and semilinear[12] passive phase conjugate mirrors, for example. It was also found that oxidation and reductions techniques served as effective methods for varying the value of $\Gamma$ in these crystals. However, the application of an external electric field to the crystals tended to degrade their optical quality rather than improve the value of their coupling coefficients.

The response times of the SBN crystals we tested averaged about 100 msec for an incident irradiance of 1W/cm$^2$. In general, SBN:Ce responded quicker than SBN:60 with times approaching 50 msec at 1W/cm$^2$. Since the two beam-coupling coefficient of SBN:Ce is so large, the time required to reach a given diffraction efficiency with SBN:Ce will, therefore, be much shorter than that needed with SBN:60. Although the response time of SBN:Fe has yet to be reliably determined, we believe that its speed will not significantly differ from that of the other two crystals.

## Conclusion

High optical quality undoped and doped single crystal SBN:60 has been grown and proven to be photorefractive. This effect was quantified by measuring the coupling coefficients and response times of several samples using the method of two-wave mixing. The results of this work indicate that the introduction of dopants into SBN:60 produce crystals with an even greater photorefractive effect than that of undoped SBN:60.

## Acknowledgements

This research was supported by grants from Rockwell International Corporation, the U. S. Air Force Office of Scientific Research and the U.S. Army Research Office.

## References

1. Jamieson, P. B., Abrahams, S. C., and Bernstein, J. L., J. Chem. Phys, Vol. 48, 5048. 1968.
2. Jamieson, P. B., Abrahams, S. C., and Bernstein, J. L., J. Chem. Phys, Vol. 50, 4352. 1969.
3. Abrahams, S. C., Jamieson, P. B., Bernstein, J. L., J. Chem. Phys, Vol. 54, 2355. 1971.

4. Kaminow, I. P., and Turner, E. H., Handbook of Lasers with Selected Data on Optical Technology, the Chemical Rubber Co., 447. 1971.
5. Valley, G. C., Klein, M. B., Opt. Eng., Vol. 22, 7. 704. 1983.
6. Kukhtarev, N. V., Markov, V. B., and Odulov, S. G., Opt. Comm., Vol. 23, 338. 1977.
7. Kukhtarev, N. V., Markov, V. B., Odulov, S. G., Soskin, M. S., and Vinetskii, V. L., Ferroelectrics, Vol. 22, 949. 1979.
8. Kukhtarev, N. V., Sov. Tech. Phys. Lett., Vol. 2, 438. 1976.
9. Rakuljic, G. A., Yariv, A., Neurgaonkar, R. R., "Application of the Band Transport Model to Photorefractive Strontium Barium Niobate," 1984.
10. Phillips, W., Amodei, J. J., Staebler, D. L., RCA Review, Vol. 33, 94. 1972.
11. Cronin-Golomb, M., Fischer, B., White, J. O., and Yariv, A., Appl. Phys. Lett., Vol. 42, 919. 1983.
12. Cronin-Golomb, M., Fischer, B., White, J. O., Yariv, A., Appl. Phys. Lett., Vol. 41, 689. 1982.

**Table 1: Elemental Analysis by Weight of SBN:60 and SBN:Ce**

| Elements & Units | SBN:60 | SBN:Ce |
|---|---|---|
| U PPM | < 0.1 | < 0.1 |
| TH PPM | < 0.3 | < 0.2 |
| NA PPM | 30.0 | <30.0 |
| SC PPM | 0.04 | 0.04 |
| CR PPM | < 5.0 | < 5.0 |
| FE % | 0.029 | 0.014 |
| CO PPM | 0.3 | 0.3 |
| NI PPM | 50.0 | 50.0 |
| ZN PPM | 7.0 | 5.0 |
| AS PPM | < 1.0 | < 1.0 |
| SE PPM | < 5.0 | < 5.0 |
| BR PPM | < 0.5 | < 0.5 |
| MO PPM | 11.0 | 4.0 |
| SB PPM | 0.5 | 0.5 |
| CS PPM | < 0.2 | < 0.2 |
| BA PPM | 160000.0 | 150000.0 |
| LA PPM | 0.2 | 1.0 |
| HF PPM | < 0.2 | < 0.2 |
| TA PPM | 12.0 | 13.0 |
| W PPM | < 3.0 | 1.0 |
| AU PPB | < 5.0 | 5.0 |
| CE PPM | < 1.0 | 47.0 |
| ND PPM | Interfer | Interfer |
| SM PPM | 0.01 | 0.32 |
| EU PPM | 0.07 | 0.10 |
| TB PPM | < 0.1 | < 0.1 |
| YB PPM | < 0.05 | 0.05 |
| LU PPM | < 0.01 | < 0.01 |
| SR PPM | 148000.0 | 135000.0 |
| RB PPM | < 5.0 | < 5.0 |

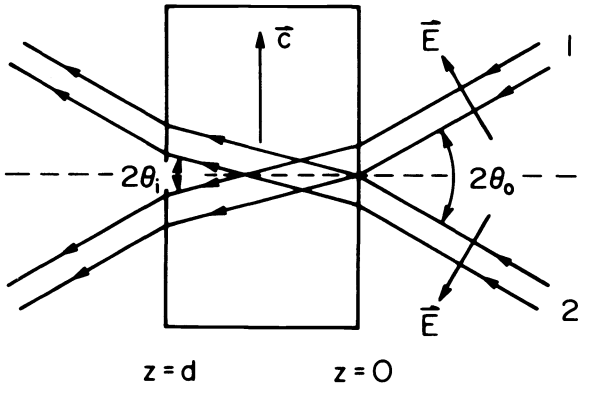


Figure 1: Experimental set-up for Two-Beam Coupling Experiments

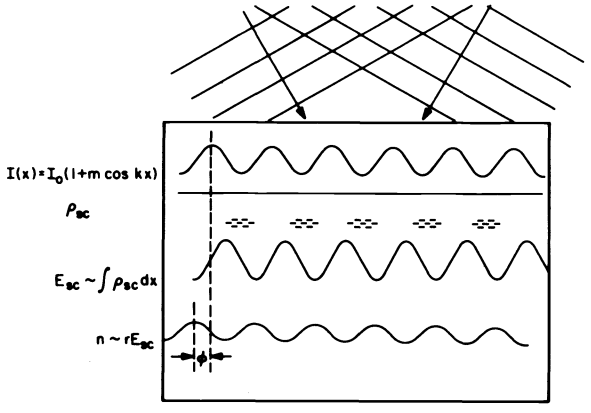


Figure 2: The Photorefractive Mechanism Two laser beams intersect, forming an interference pattern. Charge is excited where the intensity is large and migrates to regions of low intensity. The electric field associated with the resultant space charge operates through the electrooptic coefficients to produce a refractive index grating

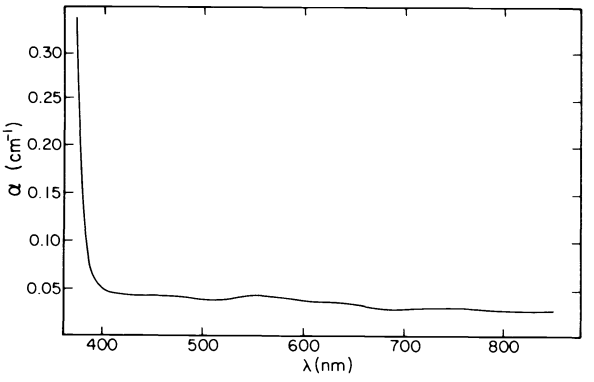


Figure 3: Absorption spectra of SBN:60

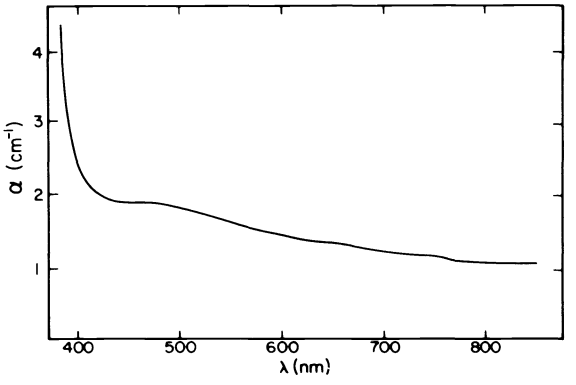


Figure 4: Absorption spectra of SBN:Ce

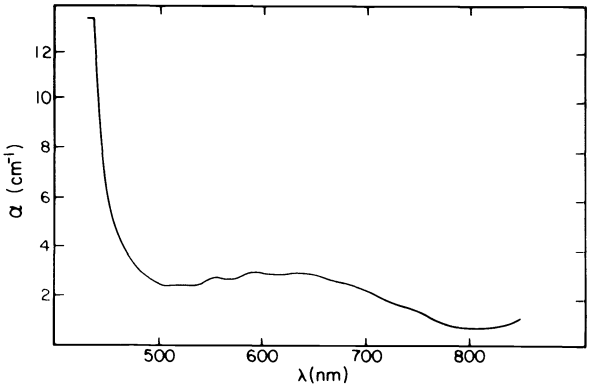


Figure 5: Absorption spectra of SBN:Fe

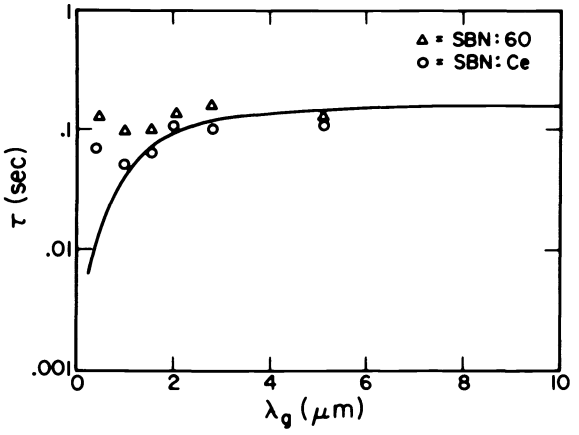


Figure 6: Response time vs. grating wavelength for $E_o$ = OV/cm

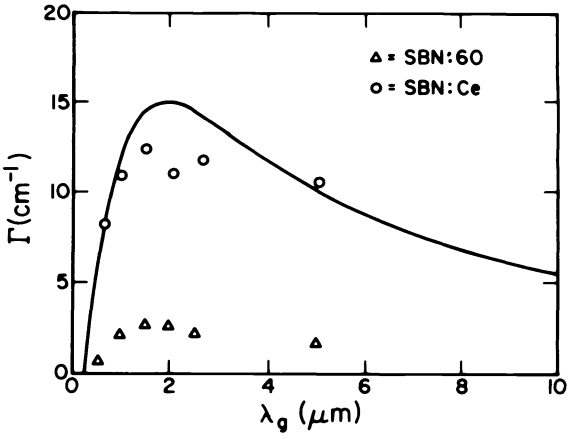


Figure 7: Coupling coefficient vs. grating wavelength for $E_o$ = OV/cm

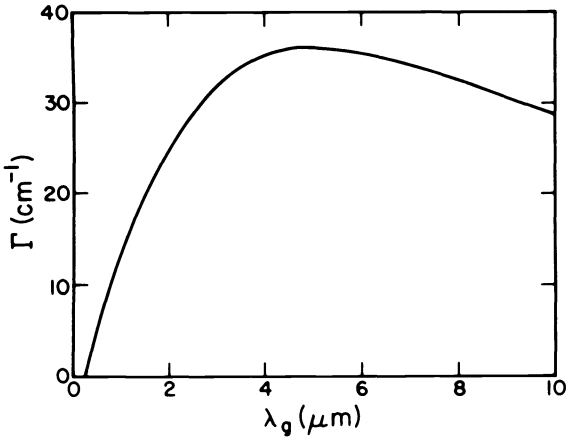


Figure 8: Coupling coefficient vs. grating wavelength for $E_o$ = 2kV/cm

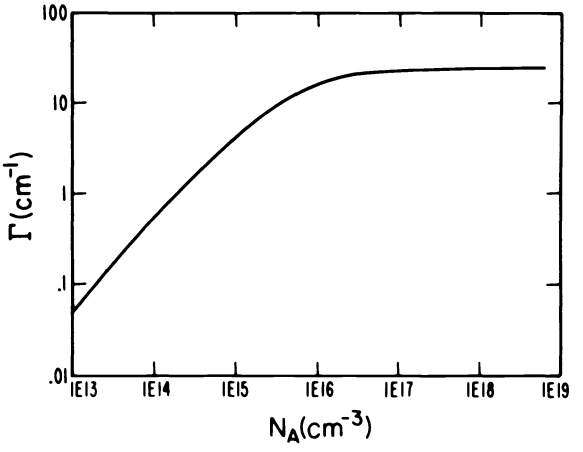


Figure 9: Coupling coefficient vs. trap density

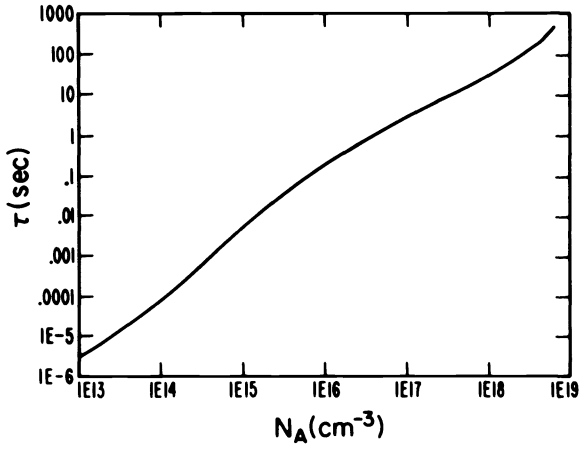


Figure 10: Response time vs. trap density

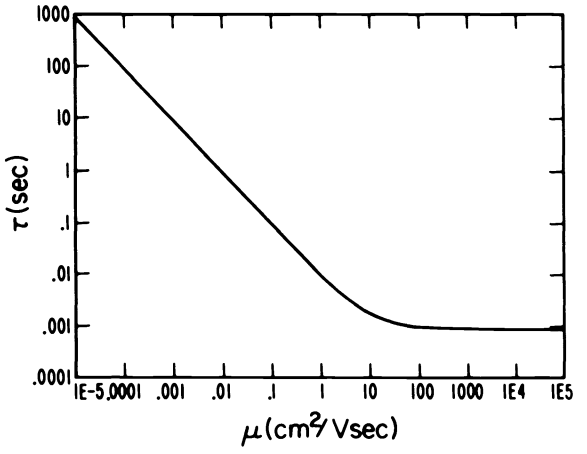


Figure 11: Response time vs. electron mobility

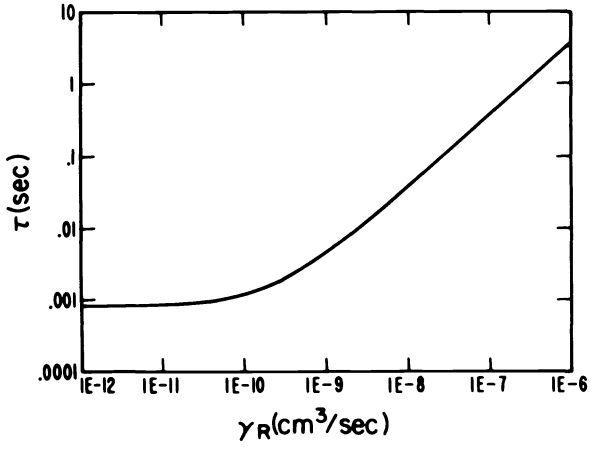


Figure 12: Response time vs. two-body recombination rate coefficient

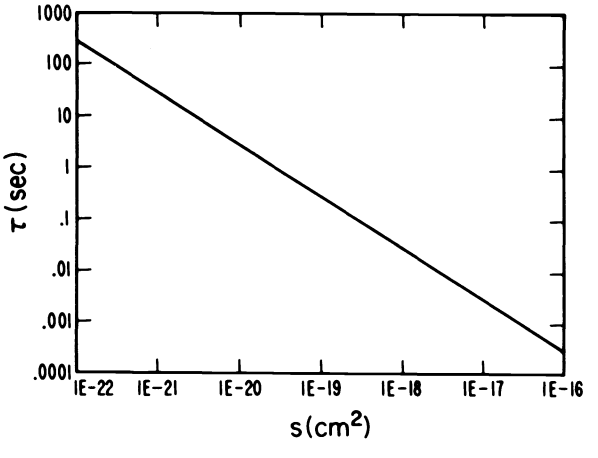


Figure 13: Response time vs. photoionization cross-section